

The Effect of Electron Distribution Function Anisotropy on Space Charge Saturated Sheath Critical Parameters in Hall Thrusters

IEPC-2009-132

*Presented at the 31st International Electric Propulsion Conference,
University of Michigan • Ann Arbor, Michigan • USA
September 20 – 24, 2009*

Daren Yu¹, Shaowei Qing², Yongjie Ding³
Lab of Plasma Propulsion, Harbin Institute of Technology, Harbin, Heilongjiang 150001, China

Xiaogang Wang⁴
State Key Lab of Nuclear Physics & Technology, School of Physics, Peking University, Beijing 100871, China

Abstract: The effect of secondary electron average kinetic energy akT_e on space charge saturated sheath critical parameters, such as wall potential ϕ_{0c} , ion energy E_c at sheath boundary and secondary electron emission yield Γ_c is investigated analytically for arbitrary single-species and isotropic plasma case by assuming a isotropy Maxwellian secondary electron velocity distribution, based on the early work of Hobbs and Wesson. Analytic results show that, as the increase of coefficient a , the critical parameters such as E_c and Γ_c are increased, while the sheath potential drop $|\phi_{0c}|$ is decreased remarkably and thereby, enhances primary electron flux and electron energy loss at wall. Also the emitted electron energy coefficient a for some high secondary electron emission (SEE) yield materials such as BN and Al_2O_3 ceramics are calculated approximately to evaluate the revised SCS sheath critical parameters. It is shown that the SCS sheath critical parameters for these high SEE yield materials are apparently different from the classical values of Hobbs and Wesson. Then, the effect of plasma electron distribution function (EDF) anisotropy caused in HTs' vertical electromagnetic field environment on the energy coefficient a is revealed for further. The effect of anisotropic EDF on energy coefficient a is formulized definitely, and it is shown that plasma EDF anisotropy can remarkably enhance the energy coefficient a and thereby, influence the plasma-wall interaction process.

Nomenclature

ϕ_0	=	wall potential
E	=	ion energy at sheath boundary
Γ	=	the total secondary electron emission coefficient
σ	=	the secondary electron emission coefficient caused by single incident electron
T_e	=	isotropy plasma electron temperature

¹ Professor, Department for Energy Science and Engineering, yudaren@hit.edu.cn.

² Doctor, Department for Energy Science and Engineering, qsw_0123@163.com.

³ Doctor, Department for Energy Science and Engineering, dingyongjie@hcms.hit.edu.cn.

⁴ Professor, Theory Department, xgwang@pking.edu.cn.

$T_{e\parallel}$	=	electron temperature parallel to magnetic field
$T_{e\perp}$	=	electron temperature vertical to magnetic field
K	=	EDF anisotropy coefficient
ε_d	=	electron drift energy
$\bar{\varepsilon}_s$	=	average kinetic energy of emitted electrons in SCS regime
ε_p	=	the energy of primary electron
k	=	the Boltzmann constant
a	=	secondary electron energy coefficient
e	=	electron charge
B_r	=	radial magnetic field
E_z	=	axial electric field
r_L	=	electron's Larmor radius

I. Introduction

The wall secondary electron emission reduces sheath potential drop¹⁻³ and, thereby weakens the thermal insulating properties of the sheath¹. As the wall secondary electron emission (SEE) yield increases to a critical value Γ_c , the sheath goes into space charge saturated (SCS) regime. At this critical point, the flux of secondary electrons from the wall reaches maximum (nearly equal to the primary electron flux), and the wall acts as an extremely effective electron energy sink. At present, the occurrence of the SCS regime has been suggested in Hall Thrusters (HTs), and extensive investigations of SCS regime in HTs have been made due to its significant effect on the performance of HTs⁴⁻¹⁴. According to these studies, electron temperature saturation and electron cooling in discharge channel are caused due to enhanced electron energy losses on the walls in the SCS regime. It is also believed that the wall SEE can enhance the electron cross-field diffusion (so-called near-wall conductivity (NWC)¹⁵). Moreover, Barral *et al.* predicted that the NWC is dominant in the SCS regime⁴. In addition, the SCS sheath also exists in other plasma application fields, such as fusion devices¹⁶, emissive walls^{2,3} and dusty plasmas¹⁷. It is obvious that, the SCS sheath has been the subject of many studies due to its relevance to plasma application fields.

The SCS sheath regime caused by wall SEE was first predicted in the original work of Hobbs and Wesson¹. According to their study, the emitted electron energy at wall is negligible ($\ll kT_e$). However, many studies have revealed that, in the process of electron-wall interaction, not only the true secondary electrons with low energy, but also the elastic reflection electrons with relatively high energy can be produced^{18,19,20}. The elastic reflection yield is in general higher at low incident electron energy for dielectrics and graphite than for metals, and rapidly increases below 30eV incident electron energy up to a value of the order of 0.5 at approximately 5-10eV incident electron energy⁴. As for the modern electric propulsion devices, such as HTs that actually work in a plasma environment with maximum electron temperature around 10-30eV, and the widely used BN ceramic wall material has high elastic reflection characteristic. Moreover, Ahedo *et al.* have predicted that the elastic reflected electrons from the channel walls can significantly reduce the sheath potential drop and, thereby enhance the fluxes of primary and secondary electrons at the walls of HTs⁷. In addition, existing fluid models have shown a significant quantitative disagreement between the prediction of the models^{4,5} and the experimental results^{11,12} with respect to the SCS regime in HTs. In their simulations, the applied SCS sheath critical parameters are the classical values of Hobbs and Wesson¹, namely wall potential $\phi_{0c} = -1.02kT_e$ and SEE yield $\Gamma_c = 0.983$. So, the assumption of negligible emitted electron energy may be not applicable for materials with high SEE characteristic.

On the one hand, this paper intends to investigate the effect of secondary electron average kinetic energy akT_e on the critical parameters of SCS sheath analytically for arbitrary single-species isotropy plasma with an assumption that the secondary electron obeys isotropy Maxwellian velocity distribution (T_e is the temperature of plasma electron, and a is the energy coefficient of secondary electrons), and to evaluate the revised SCS sheath critical parameters by calculating the emitted electron energy coefficient a approximately. On the other hand, this paper intends to reveal

the effect of plasma electron distribution function (EDF) anisotropy caused in HTs' vertical electromagnetic field environment on secondary electron energy coefficient a and SCS sheath critical parameters for further.

The paper is organized as follows. In section II, the analytic results of SCS sheath critical parameters versus the emitted electron energy coefficient a for arbitrary single-species isotropy plasma are obtained. In section III, the effect of EDF anisotropy caused in HTs' vertical electromagnetic field environment on secondary electron energy coefficient a and SCS sheath critical parameters is revealed. The energy coefficient a of emitted electrons for both isotropy and anisotropy plasma are discussed in section IV. The conclusions are summarized in section V.

II. Revision of the SCS sheath critical parameters for the isotropic plasma electron

The actual energy spectrum of secondary electrons Produced by single primary electron is very complex and present a double-peak distribution^{18,19}, while the total secondary electron energy distribution caused by primary Maxwellian²¹ or even non-Maxwellian⁷ distribution plasma electrons presents a single-peak distribution which similar to Maxwellian distribution. So, in order to make the analytic derivation more definite and executable, we only consider the energy distribution of all emitted electrons, and don't take into account of the effect of the secondary electron energy spectrum caused by single primary electron. Below, the SCS sheath critical parameters are obtained with the assumptions that the emitted electron obeys isotropy Maxwellian velocity distribution^{22,23}.

Consider an infinite plane wall, situated at $x = 0$, and the half-space $x > 0$ filled with single-species plasma. The electrostatic potential obeys Poisson's equation

$$\frac{d^2\phi}{dx^2} = 4\pi e(n_{e1} + n_{e2} - n_i).$$

where n_{e1} and n_i are the density of plasma electrons and ions respectively, and the density of emission electrons is n_{e2} , the potential at sheath boundary is $\phi(\infty) = 0$.

Assume the plasma electron obeys Maxwellian distribution and the electron temperature is T_e , then the electron density can be written

$$n_{e1} = [n_0 - n_{e2}(\infty)] \exp(e\phi / kT_e).$$

where $n_0 \equiv n_i(\infty)$, and the charge neutrality at sheath boundary ($x \rightarrow \infty$) is assumed.

The ions are assumed to be cold and to arrive at the sheath boundary with an energy $E = Mv_0^2 / 2$. The ions fall freely to the wall and their density obeys the continuity equation

$$n_i = n_0 \left(\frac{E}{E - e\phi} \right)^{1/2}.$$

Referring to Ref. 22 and 23, we assume that the emitted electron obeys semi-Maxwellian velocity distribution

$$f_0(V_0) = N \left(\frac{m}{2\pi(2akT_e)} \right)^{1/2} \exp\left(-\frac{mV_0^2}{2(2akT_e)}\right), \quad V_0 > 0,$$

where $2akT_e$ is the emitted electron temperature, $a > 0$

With the condition that the total current at wall is zero, namely $\int_0^\infty V_0 f_0(V_0) dV_0 = \frac{\Gamma}{1-\Gamma} n_0 v_0$, we obtain

$$N = \sqrt{4\pi}n_0 \frac{\Gamma}{1-\Gamma} \left(\frac{m}{M}\right)^{1/2} \left(\frac{E}{2akT_e}\right)^{1/2}.$$

Then, the emitted electron density n_{e2} can be obtained by the continuity equation and energy conservation equation for emitted electrons

$$\begin{aligned} n_{e2} &= \int_{\sqrt{\frac{2e(\phi-\phi_0)}{m}}}^{\infty} f_x(V_x) dV_x = \int_{\sqrt{\frac{2e(\phi-\phi_0)}{m}}}^{\infty} f_0 \left(\sqrt{V_x^2 - \frac{2e(\phi-\phi_0)}{m}} \right) dV_x \\ &= \frac{N}{2} \operatorname{erfc} \left(\sqrt{\frac{e(\phi-\phi_0)}{2akT_e}} \right) \exp \left(\frac{e(\phi-\phi_0)}{2akT_e} \right) \end{aligned}$$

where the complementary error function is defined by

$$\operatorname{erfc}(y) = 1 - \frac{2}{\sqrt{\pi}} \int_0^y e^{-t^2} dt,$$

Poisson's equation can be written as

$$\begin{aligned} \frac{d^2\phi}{dx^2} &= 4\pi n_0 e \left\{ \left[1 - \sqrt{\pi} \frac{\Gamma}{1-\Gamma} \left(\frac{m}{M}\right)^{1/2} \left(\frac{E}{2akT_e}\right)^{1/2} \operatorname{erfc} \left(\sqrt{\frac{-e\phi_0}{2akT_e}} \right) \exp \left(-\frac{e\phi_0}{2akT_e} \right) \right] \exp \left(\frac{e\phi}{kT_e} \right) \right. \\ &\quad \left. + \sqrt{\pi} \frac{\Gamma}{1-\Gamma} \left(\frac{m}{M}\right)^{1/2} \left(\frac{E}{2akT_e}\right)^{1/2} \exp \left(\frac{-e\phi_0}{2akT_e} \right) \operatorname{erfc} \left(\sqrt{\frac{e(\phi-\phi_0)}{2akT_e}} \right) \exp \left(\frac{e\phi}{2akT_e} \right) - \left(\frac{E}{E-e\phi} \right)^{1/2} \right\}. \end{aligned}$$

Multiplying by $d\phi/dx$ from ∞ to x , we obtain the expression

$$\begin{aligned} \frac{1}{8\pi n_0 kT_e} \left(\frac{d\phi}{dx} \right)^2 &= \frac{2E}{kT_e} \left[\left(1 - \frac{e\phi}{E} \right)^{1/2} - 1 \right] + 2a\sqrt{\pi} \frac{\Gamma}{1-\Gamma} \left(\frac{m}{M}\right)^{1/2} \left(\frac{E}{2akT_e}\right)^{1/2} \exp \left(\frac{-e\phi_0}{2akT_e} \right) \\ &\times \left[\exp \left(\frac{e\phi}{2akT_e} \right) \operatorname{erfc} \left(\sqrt{\frac{e(\phi-\phi_0)}{2akT_e}} \right) - \operatorname{erfc} \left(\sqrt{\frac{-e\phi_0}{2akT_e}} \right) + \frac{2}{\sqrt{\pi}} \exp \left(\frac{e\phi_0}{2akT_e} \right) \left(\sqrt{\frac{e(\phi-\phi_0)}{2akT_e}} - \sqrt{\frac{-e\phi_0}{2akT_e}} \right) \right]. \quad (1) \\ &+ \left[1 - \sqrt{\pi} \frac{\Gamma}{1-\Gamma} \left(\frac{m}{M}\right)^{1/2} \left(\frac{E}{2akT_e}\right)^{1/2} \operatorname{erfc} \left(\sqrt{\frac{-e\phi_0}{2akT_e}} \right) \exp \left(-\frac{e\phi_0}{2akT_e} \right) \right] \left(\exp \left(\frac{e\phi}{kT_e} \right) - 1 \right) \end{aligned}$$

We shall determine E and ϕ_0 , using the two basic condition of a steady state sheath. Firstly, the total current at wall is zero

$$\begin{aligned} & \frac{1}{4} \left[1 - \sqrt{\pi} \frac{\Gamma}{1-\Gamma} \left(\frac{m}{M} \right)^{1/2} \left(\frac{E}{2akT_e} \right)^{1/2} \operatorname{erfc} \left(\sqrt{\frac{-e\phi_0}{2akT_e}} \right) \exp \left(-\frac{e\phi_0}{2akT_e} \right) \right] \exp \left(\frac{e\phi_0}{kT_e} \right) \left(\frac{8kT_e}{\pi m} \right)^{1/2} \\ &= \frac{1}{1-\Gamma} \left(\frac{2E}{M} \right)^{1/2} \end{aligned} \quad (2)$$

Secondly, the charge neutrality condition at sheath boundary. With the Taylor expression method used in Ref. 1 and 24, we obtain an analogous result

$$\begin{aligned} E &= \frac{kT_e}{2} + \sqrt{\pi} (2a-1) kT_e \frac{\Gamma}{1-\Gamma} \left(\frac{m}{M} \right)^{1/2} \left(\frac{E}{2akT_e} \right)^{3/2} \operatorname{erfc} \left(\sqrt{\frac{-e\phi_0}{2akT_e}} \right) \exp \left(-\frac{e\phi_0}{2akT_e} \right) \\ &\quad - \frac{e\phi_0}{2a} \frac{\Gamma}{1-\Gamma} \left(\frac{m}{M} \right)^{1/2} \left(\frac{E}{-e\phi_0} \right)^{3/2} \end{aligned} \quad (3)$$

We can obtain the precise estimate of E and ϕ_0 through solving Eqs. (2) and (3). Particularly, when $(m/M)^{1/2}$ is sufficient small, we can obtain the approximate solution of E and ϕ_0

$$\left. \begin{aligned} -e\phi_0 &\simeq kT_e \ln \left[\frac{1-\Gamma}{\sqrt{2\pi m/M}} \right] \\ E &\simeq kT_e / 2 \end{aligned} \right\} \quad (4)$$

It is obvious that the electron emission leads to a reduction of the wall sheath potential drop $|\phi_0|$. When $\Gamma \rightarrow 1$, these approximate solutions break down. Before this point is reached, however a new phenomenon becomes important actually.

Using Eqs. (1) and (3) the electric field at the wall can be written

$$\begin{aligned} \frac{1}{8\pi n_0 kT_e} \left(\frac{d\phi}{dx} \right)_0^2 &= \frac{2E}{kT_e} \left[\left(1 - \frac{e\phi_0}{E} \right)^{1/2} - 1 \right] + \frac{\sqrt{\pi} (akT_e - E) \operatorname{erfc} \left(\sqrt{\frac{-e\phi_0}{2akT_e}} \right) \exp \left(-\frac{e\phi_0}{2akT_e} \right) + E \sqrt{\frac{2akT_e}{-e\phi_0}}}{\sqrt{\pi} (2a-1) \operatorname{erfc} \left(\sqrt{\frac{-e\phi_0}{2akT_e}} \right) \exp \left(-\frac{e\phi_0}{2akT_e} \right) + \sqrt{\frac{2akT_e}{-e\phi_0}}} \\ &\times \frac{1}{E} \left[\exp \left(\frac{e\phi_0}{kT_e} \right) - 1 \right] + \frac{\sqrt{\pi} 2a^2 (2E - kT_e) \exp \left(-\frac{e\phi_0}{2akT_e} \right)}{\sqrt{\pi} (2a-1) \operatorname{erfc} \left(\sqrt{\frac{-e\phi_0}{2akT_e}} \right) \exp \left(-\frac{e\phi_0}{2akT_e} \right) + \sqrt{\frac{2akT_e}{-e\phi_0}}} \\ &\times \frac{1}{E} \left[\left(1 - \frac{2}{\sqrt{\pi}} \sqrt{\frac{-e\phi_0}{2akT_e}} \right) \exp \left(\frac{e\phi_0}{2akT_e} \right) - \operatorname{erfc} \left(\sqrt{\frac{-e\phi_0}{2akT_e}} \right) \right] \end{aligned} \quad (5)$$

We may use the approximate solutions (4) to investigate the behavior of Eqs. (5) which becomes

$$\frac{1}{8\pi n_0 kT_e} \left(\frac{d\phi}{dx} \right)_0^2 \approx \left(1 - 2 \frac{e\phi_0}{kT_e} \right)^{1/2} - 2.$$

Thus, as Γ increases towards unit, the sheath potential drop $|\phi_0|$ and the electric field at wall decrease. The above equation also suggests that the electric field becomes zero for $e\phi_0 \approx -3kT_e/2$ and $\Gamma = \Gamma_c$, where Γ_c is close to but less than unit. For $\Gamma > \Gamma_c$, the monotonic solution of ϕ doesn't exist, and a potential well forms near the wall such that fraction of the emitted electrons are returned to the wall in order to maintain the effective Γ equal to Γ_c . Under these conditions, based on Hobbs and Wesson's work¹, the emission current is space-charge limited.

In order to obtain the precise solution of Γ_c , we eliminate Γ between Eqs. (2) and (3), and gain Eq. (6). Substituting $(d\phi/dx)_0 = 0$ into Eq. (5), we gain Eq. (7).

$$\frac{\sqrt{\pi} (akT_e - E_c) \operatorname{erfc} \left(\sqrt{\frac{-e\phi_{0c}}{2akT_e}} \right) \exp \left(-\frac{e\phi_{0c}}{2akT_e} \right) + E_c \sqrt{\frac{2akT_e}{-e\phi_{0c}}} \frac{1}{E_c} \exp \left(\frac{e\phi_{0c}}{kT_e} \right)}{\sqrt{\pi} (2a-1) \operatorname{erfc} \left(\sqrt{\frac{-e\phi_{0c}}{2akT_e}} \right) \exp \left(-\frac{e\phi_{0c}}{2akT_e} \right) + \sqrt{\frac{2akT_e}{-e\phi_{0c}}}} \quad (6)$$

$$= \left(\frac{m}{M} \right)^{1/2} \sqrt{\frac{4\pi E_c}{kT_e}} + \frac{a\sqrt{8a}\sqrt{\pi} (2E_c - kT_e)}{\sqrt{\pi} (2a-1) \operatorname{erfc} \left(\sqrt{\frac{-e\phi_{0c}}{2akT_e}} \right) \exp \left(-\frac{e\phi_{0c}}{2akT_e} \right) + \sqrt{\frac{2akT_e}{-e\phi_{0c}}}} \frac{1}{E_c}$$

$$0 = \frac{2E_c}{kT_e} \left[\left(1 - \frac{e\phi_{0c}}{E_c} \right)^{1/2} - 1 \right] + \frac{\sqrt{\pi} (akT_e - E_c) \operatorname{erfc} \left(\sqrt{\frac{-e\phi_{0c}}{2akT_e}} \right) \exp \left(-\frac{e\phi_{0c}}{2akT_e} \right) + E_c \sqrt{\frac{2akT_e}{-e\phi_{0c}}}}{\sqrt{\pi} (2a-1) \operatorname{erfc} \left(\sqrt{\frac{-e\phi_{0c}}{2akT_e}} \right) \exp \left(-\frac{e\phi_{0c}}{2akT_e} \right) + \sqrt{\frac{2akT_e}{-e\phi_{0c}}}}$$

$$\times \frac{1}{E_c} \left[\exp \left(\frac{e\phi_{0c}}{kT_e} \right) - 1 \right] + \frac{\sqrt{\pi} 2a^2 (2E_c - kT_e) \exp \left(-\frac{e\phi_{0c}}{2akT_e} \right)}{\sqrt{\pi} (2a-1) \operatorname{erfc} \left(\sqrt{\frac{-e\phi_{0c}}{2akT_e}} \right) \exp \left(-\frac{e\phi_{0c}}{2akT_e} \right) + \sqrt{\frac{2akT_e}{-e\phi_{0c}}}} \quad (7)$$

$$\times \frac{1}{E_c} \left[\left(1 - \frac{2}{\sqrt{\pi}} \sqrt{\frac{-e\phi_{0c}}{2akT_e}} \right) \exp \left(\frac{e\phi_{0c}}{2akT_e} \right) - \operatorname{erfc} \left(\sqrt{\frac{-e\phi_{0c}}{2akT_e}} \right) \right]$$

For certain single-species plasma, namely the mass ratio of electron to ion m/M is known, we can obtain the precise solutions of $e\phi_{0c}$ and E_c by solving Eqs. (6) and (7). Let $x = E_c/kT_e$, $y = e\phi_{0c}/E_c$, we obtain the simplified forms

$$\begin{aligned}
& \frac{\sqrt{\pi}(a-x) \operatorname{erfc}\left(\sqrt{-\frac{1}{2a}xy}\right) \exp\left(-\frac{1}{2a}xy\right) + x\sqrt{-\frac{2a}{xy}}}{\sqrt{\pi}(2a-1) \operatorname{erfc}\left(\sqrt{-\frac{1}{2a}xy}\right) \exp\left(-\frac{1}{2a}xy\right) + \sqrt{-\frac{2a}{xy}}x} \frac{1}{x} \exp(xy) \\
& = \left(\frac{m}{M}\right)^{1/2} \sqrt{4\pi x} + \frac{a\sqrt{8a}\sqrt{\pi}(2x-1)}{\sqrt{\pi}(2a-1) \operatorname{erfc}\left(\sqrt{-\frac{1}{2a}xy}\right) \exp\left(-\frac{1}{2a}xy\right) + \sqrt{-\frac{2a}{xy}}x} \frac{1}{x}
\end{aligned} \tag{8}$$

$$\begin{aligned}
0 & = 2x\left[(1-y)^{1/2} - 1\right] + \frac{\sqrt{\pi}(a-x) \operatorname{erfc}\left(\sqrt{-\frac{1}{2a}xy}\right) \exp\left(-\frac{1}{2a}xy\right) + x\sqrt{-\frac{2a}{xy}}}{\sqrt{\pi}(2a-1) \operatorname{erfc}\left(\sqrt{-\frac{1}{2a}xy}\right) \exp\left(-\frac{1}{2a}xy\right) + \sqrt{-\frac{2a}{xy}}x} \\
& \times \frac{1}{x} \left[\exp(xy) - 1\right] + \frac{\sqrt{\pi}2a^2(2x-1) \exp\left(-\frac{1}{2a}xy\right)}{\sqrt{\pi}(2a-1) \operatorname{erfc}\left(\sqrt{-\frac{1}{2a}xy}\right) \exp\left(-\frac{1}{2a}xy\right) + \sqrt{-\frac{2a}{xy}}x} \\
& \times \frac{1}{x} \left[\left(1 - \frac{2}{\sqrt{\pi}} \sqrt{-\frac{1}{2a}xy}\right) \exp\left(\frac{1}{2a}xy\right) - \operatorname{erfc}\left(\sqrt{-\frac{1}{2a}xy}\right) \right]
\end{aligned} \tag{9}$$

Substituting the solved x and y into Eq. (2), we obtain the precise solution of critical SEE yield

$$\Gamma_c = \frac{1 - \exp(-xy)(4\pi x)^{1/2} (m/M)^{1/2}}{1 + \sqrt{\pi} \exp\left(-\frac{1}{2a}xy\right) \left(\frac{1}{2a}x\right)^{1/2} \operatorname{erfc}\left(\sqrt{-\frac{1}{2a}xy}\right) (m/M)^{1/2}}. \tag{10}$$

In Ref. 1, the approximate solution of critical SEE yield was $\Gamma_c = 1 - 8.3(m/M)^{1/2}$. Let the solved precise solution of critical SEE yield $\Gamma_c = 1 - \delta(m/M)^{1/2}$.

Then, the critical parameters of SCS sheath such as ϕ_{0c} , E_c , Γ_c and δ are calculated with respect to infinite massive ions ($m/M = 0$), the Xenon, krypton, Argon, Neon, Helium and Hydrogen plasma. All the calculation results are shown in Fig. 1, from which we can see that, as the increase of the energy coefficient a , the wall potential ϕ_{0c} and ion energy E_c at sheath boundary increase sharply when a is slightly larger than zero, while δ decrease sharply when a is slightly larger than zero.

Fig. 1(a) shows that, as a increase from 0 to 0.5, the wall potential ϕ_{0c} increase from -1 to -0.4 approximately, resulting in the flux of incident electrons at wall increases to 1.86 times. As for a certain value of a , the kind of single-species plasma is a significant effect factor on ϕ_{0c} , and a light ion mass means a large wall potential ϕ_{0c} , all the curves lie between the Hydrogen and infinite massive ion. The fitted formula about the data of wall potential ϕ_{0c} (kT_e/e) versus different a is

$$\phi_{0c} = c_1 \exp(c_2 a) + c_3 \exp(c_4 a) \quad (11)$$

As the ion mass decrease from the infinite massive to the mass of Hydrogen, all the value ranges of parameters in Eq. (11) are: $c_1 = -0.23 \sim -0.22$, $c_2 = -25.1 \sim -24.8$, $c_3 = -0.7662 \sim -0.7025$, $c_4 = -1.3 \sim -1.304$.

Fig. 1(b) shows that, as a increase from 0 to 0.5, the ion energy E_c at sheath boundary increase from 0.58 to 0.66 approximately. As for a certain value of a , the kind of single-species plasma has obvious effect on E_c , and a heavy ion mass means a large E_c , all the curves lie between the Hydrogen and infinite massive ion. The fitted formula about the data of ion energy E_c versus different a is

$$E_c = l_1 \exp(l_2 a) + l_3 \exp(l_4 a) \quad (12)$$

As the ion mass decrease from the infinite massive to the mass of Hydrogen, all the value ranges of parameters in Eq. (12) are: $l_1 = 0.6443 \sim 0.64$, $l_2 = 0.0617 \sim 0.05519$, $l_3 = -0.0604 \sim -0.6$, $l_4 = -12.28 \sim -12.55$.

Fig. 1(c) shows that, as a increase from 0 to 0.5, the coefficient δ decrease from 8.0 to 5.0 approximately. As for a certain value of a , the kind of single-species plasma is a significant effect factor on δ , and a large ion mass means a large coefficient δ . The fitted formula about the data of coefficient δ versus different a is

$$\delta = g_1 \exp(g_2 a) + g_3 \exp(g_4 a) \quad (13)$$

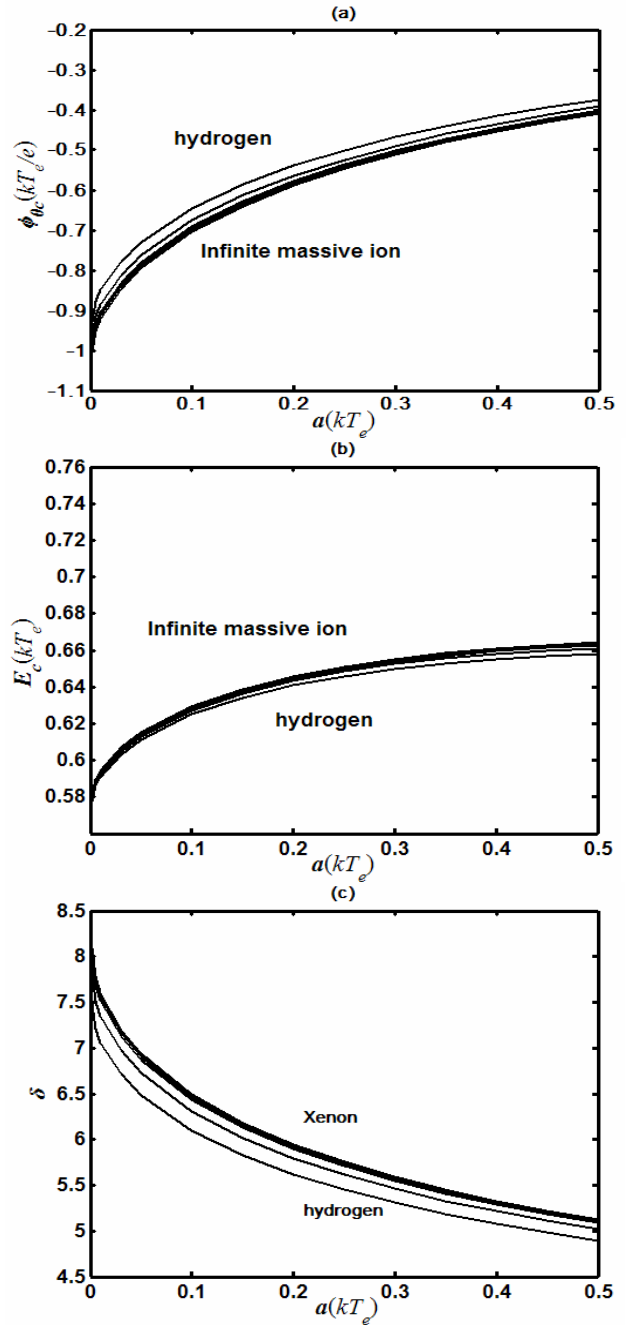


Figure 1. The analytic results about the evolution profiles of SCS sheath critical parameters versus the average kinetic energy akT_e of secondary electrons with respect to infinite massive ions ($m/M=0$), the Xenon, krypton, Argon, Neon, Helium and Hydrogen plasma, the secondary electron obeys semi-Maxwellian velocity distribution. (a) Wall potential ϕ_{0c} . (b) The ion energy at sheath boundary E_c . (c) The coefficient δ .

As the ion mass decrease from the infinite massive to the mass of Hydrogen, all the value ranges of parameters in Eq. (13) are: $g_1 = 1.414 \sim 1.22$, $g_2 = -23.89 \sim -23.22$, $g_3 = 6.634 \sim 6.214$, $g_4 = -0.5405 \sim -0.4983$.

III. The effect of EDF anisotropy on SCS sheath critical parameters in Hall Thrusters

The schematic vertical electromagnetic field in HTs is shown in Fig. 2. A magnetic field with only a radial component B_r is imposed and an axial electric field

E_z is applied. Because the electron mean free path in HTs is much larger than the channel width, the EDF in HTs' discharge channel has been shown to be strongly anisotropic and depleted at high energies^{8,9,25}. The EDF anisotropy can be explained qualitatively as follows^{9,26}. The electrons can gain energy $\Delta\epsilon = eE_z r_L$ from the axial electric field E_z as a result of turbulent collisions and collisions with neutral atoms, where r_L is the electron's Larmor

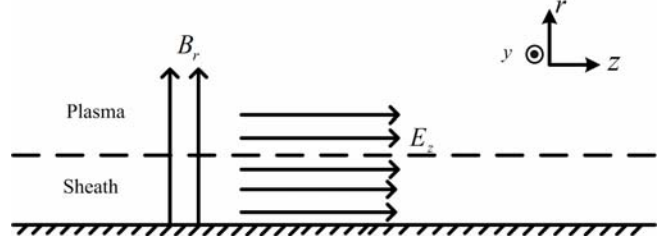


Figure 2. The schematic distribution of the vertical electromagnetic field in HTs' discharge channel.

radius. This energy increment $\Delta\epsilon$ is distributed in the direction parallel to the walls. In addition, the electron-neutral collisions tend to turn the electron toward the wall. The electrons in HTs' discharge channel can be divided into three groups. The electron with energy $\epsilon_r > e\Phi$ can quickly leave the plasma and collide with the wall, where Φ is the plasma potential relative to the wall. The electron with energy $\epsilon = \epsilon_y + \epsilon_z + \epsilon_r > e\Phi$ and $\epsilon_r < e\Phi$ can be scattered to the wall by electron-neutral collisions. Electrons with energy $\epsilon < e\Phi$ can't be scattered to the wall unless they are heated by axial electric field. The electron-neutral collisions tend to make the EDF isotropic in the energy region $\epsilon < e\Phi$, while the electron turbulent collisions tend to make the EDF anisotropic. If the electron turbulent collision frequency is much greater than electron-neutral collision frequency, the EDF should be anisotropic^{9,27}.

In order to make the evaluation of EDF anisotropy effect on SCS sheath critical parameters more definitely, we assume that the plasma electron distribution is a shifted bi-Maxwellian parameterized by $T_{e\parallel}$, $T_{e\perp}$ and ϵ_d , where $T_{e\parallel}$ and $T_{e\perp}$ are the electron temperature parallel to magnetic field and vertical to magnetic field respectively, ϵ_d is the electron drift energy⁴.

We assume that the electron and ion in sheath region are collisionless, considering that the sheath is very thin. The results about the modified SCS sheath critical parameters for isotropic Maxwellian distribution plasma electron in section II is applicable in HTs' vertical electromagnetic field environment, due to the vertical electromagnetic field has no effect on the electron motion in the radial direction of near wall sheath. Then, the energy coefficient of emitted electrons in SCS regime can be written as

$$a = \bar{\epsilon}_s / kT_{e\parallel}. \quad (14)$$

where $\bar{\epsilon}_s$ is the average kinetic energy of emitted electrons in SCS regime.

Following Ref. 4, the wall SEE yield can be expressed as a linear law

$$\sigma(\epsilon_p) = \sigma(0) + \frac{\epsilon_p}{\epsilon^*} [1 - \sigma(0)]. \quad (15)$$

where ϵ_p is the energy of primary electron, and ϵ^* is the crossover energy. The effective total SEE yield Γ then can be obtained by integration of σ over the EDF at wall. With the linearity of σ , we obtain

$$\Gamma = \sigma(\bar{\varepsilon}_p). \quad (16)$$

where $\bar{\varepsilon}_p$ is the mean energy of electrons impinging the wall. Without going to the detail derivation process in Ref. 4, this mean energy actually can be written as $\bar{\varepsilon}_p = kT_{e\parallel} + kT_{e\perp} + \varepsilon_d$.

As the effective total SEE yield $\Gamma = \Gamma_c \rightarrow 1$ in SCS regime, we can obtain the mean energy of primary electrons $\bar{\varepsilon}_p \approx \varepsilon^*$ at wall in SCS regime from Eqs. (15) and (16). Therefore, as for a certain wall material, the mean energy of primary electron $\bar{\varepsilon}_p \approx \varepsilon^* = \text{constant}$ and the average kinetic energy of emitted electrons $\bar{\varepsilon}_s = \text{constant}$ in SCS regime.

Then, the energy coefficient a of emitted electrons in SCS regime with considering EDF anisotropy can be written as

$$a = (1 + \mathbf{K} / 2)a_0. \quad (17)$$

where the EDF anisotropy coefficient is defined as $\mathbf{K} = (kT_{e\perp} + \varepsilon_d - kT_{e\parallel}) / kT_{e\parallel}$, and $a_0 = 2\bar{\varepsilon}_s / \varepsilon^*$ is the energy coefficient of emitted electrons corresponding to EDF isotropy ($\mathbf{K} = 0$) in SCS regime.

Based on the results of fluid simulation⁴ and kinetic studies^{8,28}, we know that the plasma electron temperature ratio $T_{e\perp} / T_{e\parallel} \approx 3 \sim 4$ under SCS regime in HTs. Thus, we can obtain the EDF anisotropy coefficient $\mathbf{K} \approx 3$ in HTs' strong EDF anisotropy condition. We can see that the EDF anisotropy phenomenon can significantly enhance the energy coefficient a and thereby, influence the SCS sheath critical parameters and the plasma-wall interaction process, as shown in Fig. 1.

IV. Discussion

Due to the emitted electron energy coefficient a has significant influence on SCS critical parameters and the plasma wall interaction process as shown in Fig.1, it is necessary to quantitatively evaluate the energy coefficient a of emitted electrons. In general, the energy coefficient a should be small, due to the plasma electron critical temperature is high in SCS regime and, thereby the number of elastic reflected electrons with relatively high energy is small. However, for some high emission yield dielectric wall materials such as BN and Al₂O₃ ceramics, the critical temperature of plasma electron with a Maxwellian velocity distribution is around 10~30eV⁴. In such a critical temperature, the elastic reflection electrons component can't be neglected, so we should evaluate the energy coefficient a in detail.

In order to evaluate the energy coefficient a , we shall calculate the emitted electron mean energy flux $Q_{SEEx} = \int_0^\infty \frac{1}{2} mV_0^2 V_0 f_0(V_0) dV_0 / \int_0^\infty V_0 f_0(V_0) dV_0 = 2akT_e$ in SCS regime. In general, the emitted electrons can be divided into two components, namely true secondary electrons and backscattering electrons. Then, we also can obtain the emitted electron mean energy flux Q_{SEEx} by calculating the energy flux of true secondary electron and backscattering electron respectively

$$Q_{SEEx} = \frac{\frac{1}{2} \bar{\tau} \cdot \eta J_{e1} \cdot \bar{\varepsilon}_p + \frac{1}{2} (\Gamma_c - \eta) J_{e1} \cdot \bar{\varepsilon}_{ts}}{\Gamma_c J_{e1}}. \quad (18)$$

where, $\bar{\tau}$ is the mean energy ratio between primary and backscattered electrons, this constant value can be assumed $\bar{\tau} = 0.6$ empirically⁴, η is the total backscattering yield, $\bar{\varepsilon}_p = 2kT_e$ is the mean energy of electrons impinging the wall, $\bar{\varepsilon}_{s_0} = 2eV$ is the mean energy of true secondary electrons⁷, J_{e1} is the primary electron flux.

Considering $\Gamma_c \rightarrow 1$ in SCS regime, we can obtain a simplified formula for energy coefficient a in SCS regime by assuming $\Gamma_c = 1$.

$$a = \frac{1}{2}0.6 \cdot \eta + \frac{1}{2kT_e}(1 - \eta). \quad (19)$$

This formula indicates that the energy coefficient a is generally determined by two parameters, namely the total backscattering yield η and plasma electron temperature T_e .

Following Ref. 7, the backscattering yield σ_{sr} can be expressed as

$$\sigma_{sr} = \sigma_0 \exp(-\varepsilon_p / \varepsilon_r) \quad (20)$$

where ε_p is the energy of primary electron. Typical constant values for BN ceramics used in HTs are $\sigma_0 = 0.5$, $\varepsilon_r = 50eV$ and $2kT_e = 53eV$ in SCS regime^{4,7}. Then the effective total backscattering yield η in SCS regime can be obtained by integration of σ_{sr} over the Maxwellian electron EDF at wall, namely $\eta \approx 0.2136$. Thus we obtain the emitted electron energy coefficient $a = 0.0789$ for BN ceramic.

As for a higher SEE yield material such as Al_2O_3 ceramics, the typical constant values are $\sigma_0 = 0.6$, $\varepsilon_r = 50eV$ and $2kT_e = 18eV$ in SCS regime^{4,7}. Then we obtain the effective total backscattering yield $\eta = 0.4307$. Thus we can also obtain the emitted electron energy coefficient $a = 0.1608$.

Based on Eq. (19) and the two calculation examples of emitted electron energy coefficient a for BN and Al_2O_3 ceramics above, we can see that the secondary electron energy coefficient a in the SCS regime is variable according to different materials due to their different SEE characteristics, and a wall material with high SEE yield characteristic should have a relatively large energy coefficient a in SCS regime.

Referring to Eqs. (11) and (13) for isotropy plasma electron and making use of Eqs. (17), we can obtain the modified formulas about SCS sheath critical parameters for anisotropic Xenon plasma with Maxwellian electron distribution in HTs

$$\begin{aligned} \phi_{0c} &= -\frac{kT_{ell}}{e} \left\{ 0.2331 \exp[-25.06(1 + K/2)a_0] + 0.7604 \exp[-1.296(1 + K/2)a_0] \right\}, \\ E_c &= kT_{ell} \left\{ 0.6438 \exp[0.06156(1 + K/2)a_0] - 0.05999 \exp[-12.33(1 + K/2)a_0] \right\}, \end{aligned} \quad (21)$$

$$\delta = 1.414 \exp[-23.89(1 + K/2)a_0] + 6.634 \exp[-0.5405(1 + K/2)a_0].$$

V. Conclusion

This paper has predicted the significant influence of secondary electron average kinetic energy akT_e on SCS sheath critical parameters by assuming that the secondary electron obeys semi-Maxwellian velocity distribution, based on a one-dimensional steady-state sheath model. As for some wall materials with high SEE yield characteristic such as BN and Al₂O₃ ceramics, the secondary electron energy coefficient a can't be neglected. In this condition, the SCS sheath critical parameters as shown in our analytic results are apparently different from the classical values of Hobbs and Wesson¹.

It is shown that the secondary electron energy coefficient a has significant influence on the critical parameters in SCS regime. As the increase of coefficient a , the critical parameters such as E_c and Γ_c are increased, while the sheath potential drop $|\phi_{0c}|$ is decreased remarkably and thereby, enhances primary electron flux and electron energy loss at wall. The ion mass also has its influence on the critical parameters, for a certain coefficient a , a heavy ion has a relatively low wall potential ϕ_{0c} , but has relatively high ion energy E_c and SEE yield Γ_c .

The plasma EDF anisotropy caused by a vertical electromagnetic field in HTs has significant influence on SCS sheath critical parameters and, thereby the plasma-wall interaction process. The obtained results present some understanding of plasma sheath, and the revised formulas about SCS sheath critical parameters can be applied in fluid models of plasma discharge in HTs. These conclusions can also have impact on studies for plasma discharge in related areas.

Acknowledgments

Mr. Daren Yu would like to acknowledge the NSFC Grant No. 50676026 and No. 60671012.

References

- ¹ Hobbs, G. D., and Wesson, J. A., "Heat flow through a Langmuir sheath in the presence of electron emission," *Plasma Phys*, Vol. 9, 1967, pp. 85-87.
- ² Schwager, L. A., "Effects of secondary and thermionic electron emission on the collector and source sheaths of a finite ion temperature plasma using kinetic theory and numerical simulation," *Phys. Fluids B*, Vol. 5, No. 2, 1993, pp. 631-645.
- ³ Intrator, T., Cho, M. H., Wang, E. Y., Hershkowitz, N., Diebold, D., DeKock, J., "The virtual cathode as a transient double sheath," *J. Appl. Phys*, Vol. 64, No. 6, 1988, pp. 2927-2933.
- ⁴ Barral, S., Makowski, K., Peradzynski, Z., Gascon, N., Dudeck, M., "Wall material effects in stationary plasma thrusters. II. Near-wall and in-wall conductivity," *Phys. Plasmas*, Vol. 10, No. 10, 2003, pp. 4137-4152; Gascon, N., Dudeck, M., Barral, S., "Wall material effects in stationary plasma thrusters. I. Parametric studies of an SPT-100," *Phys. Plasmas*, Vol. 10, No. 10, 2003, pp. 4123-4136.
- ⁵ Ahedo, E., Gallardo, J. M., Martinez-Sanchez, M., "Effects of the radial plasma-wall interaction on the Hall thruster discharge," *Phys. Plasmas*, Vol. 10, No. 8, 2003, pp. 3397-3409.
- ⁶ Ahedo, E., Parra, D. I., "Partial trapping of secondary-electron emission in a Hall thruster plasma," *Phys. Plasmas*, Vol. 12, 2005, pp. 073503.
- ⁷ Ahedo, E., De Pablo, V., "Combined effects of electron partial thermalization and secondary emission in Hall thruster discharges," *Phys. Plasmas*, Vol. 14, 2007, pp. 083501.
- ⁸ Sydorenko, D., Smolyakov, A., Kaganovich, I., Raites, Y., "Kinetic simulation of secondary electron emission effects in Hall thrusters," *Phys. Plasmas*, Vol. 13, 2006, pp. 014501.
- ⁹ Kaganovich, I., "Modeling of collisionless and kinetic effects in thruster plasmas," *Proceedings of the 29th International Electric Propulsion Conference*, Electric Rocket Propulsion Society, Cleveland, OH, IEPC-05 paper 096.
- ¹⁰ Keidar, M., Boyd, I. D., Beilis, I. I., "Plasma flow and plasma-wall transition in Hall thruster channel," *Phys. Plasmas*, Vol. 8, No. 12, 2001, pp. 5315-5322.
- ¹¹ Raites, Y., Staack, D., Smirnov, A., Fisch, N. J., "Space charge saturated sheath regime and electron temperature saturation in Hall thrusters," *Phys. Plasmas*, Vol. 12, 2005, pp. 073507.
- ¹² Raites, Y., Staack, D., Keidar, M., Fisch, N. J., "Electron-wall interaction in Hall thrusters," *Phys. Plasmas*, Vol. 12, 2005, pp. 057104.
- ¹³ Raites, Y., Smirnov, A., Staack, D., Fisch, N. J., "Measurements of secondary electron emission effects in the Hall thruster discharge," *Phys. Plasmas*, Vol. 13, 2006, pp. 014502.
- ¹⁴ Taccogna, F., Longo, S., Capitelli, M., "plasma sheaths in hall thrusters," *Phys. Plasmas*, Vol. 12, 2005, pp. 093506.
- ¹⁵ Morozov, A. I., and Savelev, V. V., "Theory of the Near-Wall Conductivity," *Plasma Phys. Rep*, Vol. 27, No. 7, 2001, pp. 570-575.
- ¹⁶ Stangeby, P. C., *The Plasma Boundary of Magnetic Fusion Devices*, Plasma Physics Series, IOP, Bristol, 2000, pp. 646-654.

-
- ¹⁷ Delzanno, G. L., Lapenta, G., Rosenberg, M., "Attractive Potential around a Thermionically Emitting Microparticle," *Phys. Rev. Lett.*, Vol. 92, No. 3, 2004, pp. 035002.
- ¹⁸ Seiler, H., "Secondary electron emission in the scanning electron microscope," *Journal of Applied Physics*, Vol. 54, No. 11, 1983, pp. R1.
- ¹⁹ Morozov, A. I., Savelev, V. V., *Reviews of Plasma Physics*, New York Consultants Bureau, New York, 2001, Vol. 21, PP. 241.
- ²⁰ Dunaevsky, A., Raitsev, Y., Fisch, N. J., "Secondary electron emission from dielectric materials of a Hall thruster with segmented electrodes," *Phys. Plasmas*, Vol. 10, 2003, PP. 2574.
- ²¹ Taccogna, F., Longo, S., and Capitelli, M., "Effects of secondary electron emission from a floating surface on the plasma sheath," *Vacuum*, Vol. 73, 2004, PP. 89-92.
- ²² Porter G, D., "Effect of gas recycling and secondary electron emission on the axial power flow in an open-ended device," *Nucl. Fusion*, Vol. 22, 1982, PP. 1279-1289.
- ²³ Takamura, S., Ohno, N., Ye, M. Y., Kuwabara, T., "Space-Charge Limited Current from Plasma-Facing Material Surface," *Contrib. Plasma Phys.*, Vol. 44, No. 1-3, 2004, PP. 126-137.
- ²⁴ Bohm, D., "The Characteristic of Electrical Discharge in Magnetic Fields", edited by A. Guthrie and R. K. Wakerling, McGraw-Hill, New York, 1949.
- ²⁵ Sydorenko, D., Smolyakov, A., Kaganovich, I., Raitsev, Y., "Modification of Electron Velocity Distribution in Bounded Plasmas by Secondary Electron Emission," *IEEE Trans. Plasma Sci.*, Vol. 34, 2006, PP. 815.
- ²⁶ Sydorenko, D., Smolyakov, A., Kaganovich, I., Raitsev, Y., "Kinetic Simulation of Effects of Secondary Electron Emission on Electron Temperature in Hall Thrusters," *Proceedings of the 29th International Electric Propulsion Conference*, Electric Rocket Propulsion Society, Cleveland, OH, IEPC-05 paper 078.
- ²⁷ Kaganovich, I., Misina, M., Berezhnoi, S. V., Gijbels, R., "Electron Boltzmann kinetic equation averaged over fast electron bouncing and pitch-angle scattering for fast modeling of electron cyclotron resonance discharge," *Phys. Rev. E*, Vol. 61, No. 2, 2000, PP. 1875-1889.
- ²⁸ Kaganovich, I. D., Raitsev, Y., Sydorenko, D., Smolyakov, A., "Kinetic effects in a Hall thruster discharge," *Phys. Plasmas*, Vol. 14, 2007, PP. 057104.